

Supplementary Information for “LiMg_{0.1}Co_{0.9}BO₃ as a Positive Electrode Material for Li-ion Batteries”

The Rietveld refinement has been performed with GSAS-II¹ based on the structure reported by Piffard *et al.*² The occupancy for Mg is set to 0.1 and estimated to take only Co1 positions. The atomic coordinates are also left according to the crystal structure reported by Piffard *et al.*² and no attempts to refine specific atomic positions are taken here. The results are given below:

Refinement output

Crystal data

Formula sum	B Co _{0.9} Li Mg _{0.1} O ₃
Formula weight	121.22
Crystal system	monoclinic
Space group	C 1 2/c 1 (no. 15)
Unit cell dimensions	$a = 5.1101(6) \text{ \AA}$ $b = 8.7962(8) \text{ \AA}$ $c = 10.0351(9) \text{ \AA}$ $\beta = 91.44(1)^\circ$
Cell volume	450.93(6) \AA^3
Z	8
Density, calculated	3.571 g/cm ³
Pearson code	mC64
Formula type	NOPQ3
Wyckoff sequence	f ⁸

Atomic coordinates

Atom	Wyck.	Occ.	x	y	z
Co1	8f	0.46	0.16570	0.16730	0.13250
Co2	8f	0.44	0.15470	0.16450	0.11360
Li1	8f	0.48	0.66100	0.00300	0.08800
Li2	8f	0.52	0.66300	-0.00500	0.15700
B1	8f		0.16420	-0.16840	0.12580
O1	8f		0.40260	0.33560	0.09130
O2	8f		-0.21670	0.19440	0.15870
O3	8f		0.30880	-0.03890	0.12660
Mg9	8f	0.1	0.16570	0.16730	0.13250

Anisotropic displacement parameters (in \AA^2)

Atom	U_{11}	U_{22}	U_{33}	U_{12}	U_{13}	U_{23}
O1	0.00760	0.01020	0.00820	0.00010	-0.00090	0.00090
O2	0.00650	0.00600	0.01000	0.00020	-0.00190	0.00040
O3	0.00590	0.00600	0.04000	0.00010	-0.00310	0.00000

Selected geometric parameters (\AA , $^\circ$)

Co1—Li2 ⁱ	8.709(13)	Li2—Mg9 ^{iv}	10.622(1)
Co1—O1	1.963(3)	B1—O3	1.358(0)
Co1—O2	1.993(3)	O1—Co1	1.963(3)
Co1—O2 ⁱⁱ	2.118(3)	O1—Co2	1.983(2)
Co1—O3	1.957(0)	O2—Co1	1.993(3)
Co2—Li1 ⁱⁱⁱ	8.641(13)	O2—Co1 ⁱⁱ	2.118(3)
Co2—O1	1.983(2)	O2—Co2	1.980(6)
Co2—O2	1.980(6)	O2—Li1 ^v	11.428(4)
Co2—O3	1.958(1)	O2—Li2 ^v	11.468(1)

Li1—Co2 ⁱⁱⁱ	8.641(13)	O3—Co1	1.957(0)
Li1—Li1 ⁱⁱⁱ	11.163(14)	O3—Co2	1.958(1)
Li1—Li2	0.696(0)	O3—Li1	1.887(5)
Li1—Li2 ⁱⁱⁱ	11.343(19)	O3—Li1 ⁱⁱⁱ	10.568(13)
Li1—O2 ^{iv}	11.428(4)	O3—Li2	1.852(4)
Li1—O3	1.887(5)	O3—Li2 ⁱ	10.613(13)
Li1—O3 ⁱⁱⁱ	10.568(13)	O3—B1	1.358(0)
Li1—Mg9	2.958(5)	Mg9—Li1 ^v	10.562(2)
Li1—Mg9 ^{iv}	10.562(2)	Mg9—Li1	2.958(5)
Li1—Mg9 ⁱⁱⁱ	8.691(14)	Mg9—Li1 ⁱⁱⁱ	8.691(14)
Li2—Co1 ⁱ	11.366(10)	Mg9—Li2 ^v	10.622(1)
Li2—Li1	0.696(0)	Mg9—Li2	2.964(3)
Li2—Li1 ⁱⁱⁱ	11.343(19)	Mg9—Li2 ⁱ	8.709(13)
Li2—Li2 ⁱ	11.287(15)	Mg9—O1	1.963(3)
Li2—O2 ^{iv}	11.468(1)	Mg9—O2	1.993(3)
Li2—O3	1.852(4)	Mg9—O2 ⁱⁱ	2.118(3)
Li2—O3 ⁱ	10.106(14)	Mg9—O3	1.957(0)
Li2—Mg9	2.964(3)	Mg9—Mg9 ⁱⁱ	2.938(18)
Li1 ⁱⁱⁱ —Li1—Li2	103.32(0)	Li2 ⁱ —Li2—O3	64.18(0)
Li1 ⁱⁱⁱ —Li1—O2 ^{iv}	19.03(0)	O2 ^{iv} —Li2—O3	76.52(0)
Li2—Li1—O2 ^{iv}	91.54(0)	Li1 ^v —O2—Li2 ^v	3.48(0)
Li1 ⁱⁱⁱ —Li1—O3	66.98(0)	Li1—O3—Li2	21.42(0)
Li2—Li1—O3	76.48(0)	Li1—O3—B1	133.19(0)
O2 ^{iv} —Li1—O3	77.79(0)	Li2—O3—B1	131.72(0)
Li1—Li2—Li2 ⁱ	95.27(0)	O1—Mg9—O2	123.34(0)
Li1—Li2—O2 ^{iv}	84.98(0)	O1—Mg9—O3	117.37(0)
Li2 ⁱ —Li2—O2 ^{iv}	17.42(0)	O2—Mg9—O3	118.9(0)
Li1—Li2—O3	82.1(0)		

Symmetry codes:

(i) -x, 1+y, 0.5-z; (ii) -x, y, 0.5-z; (iii) -x, 1-y, -z; (iv) x, 1+y, z;
(v) x, -1+y, z.

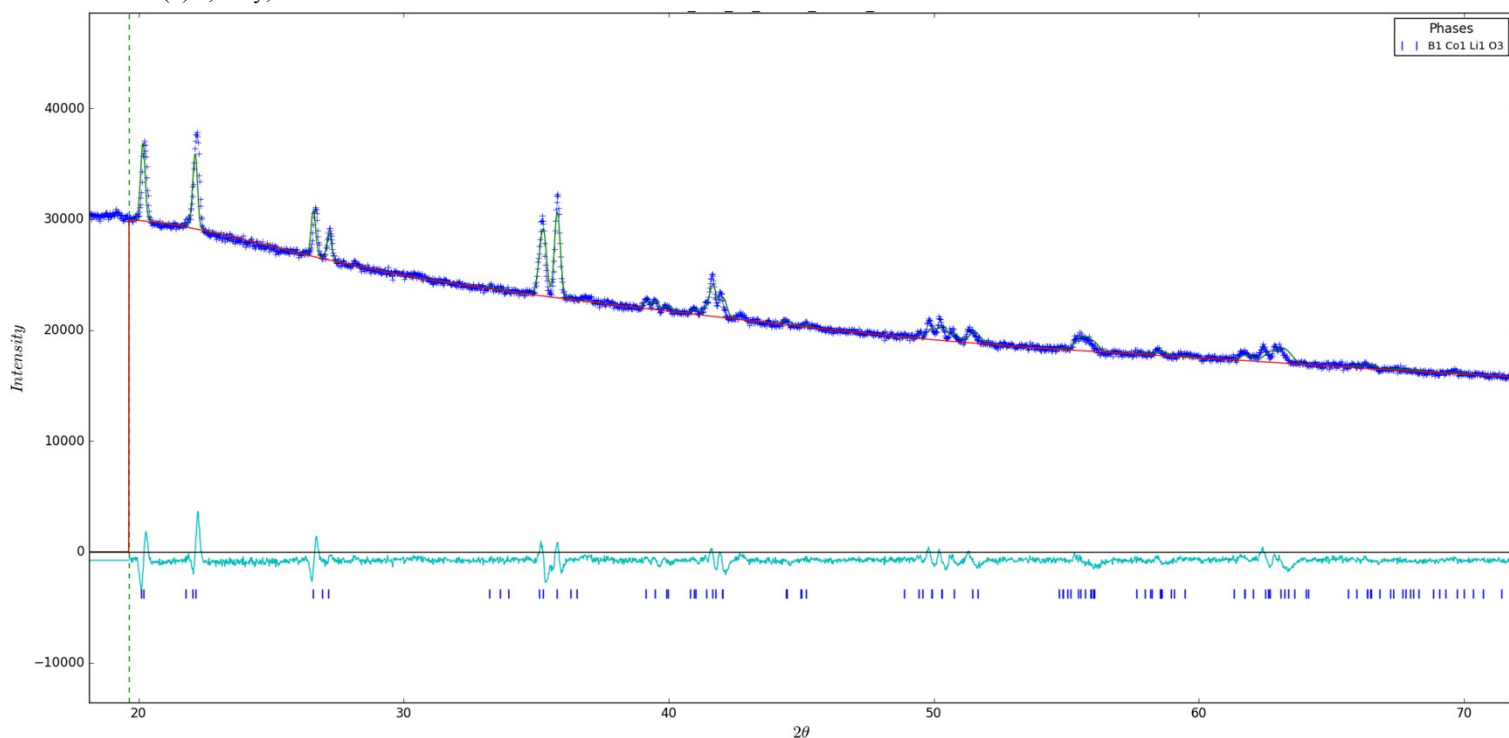


Figure S 1 The Rietveld refinement for $\text{LiMg}_{0.1}\text{Co}_{0.9}\text{BO}_3$ (done with GSAS-II¹) between 2 theta = 19.5 and 75 degrees, $wR = 1.63\%$. The blue curve corresponds to the experimental data and the green curve is the calculated fit. The bottom cyan coloured curve is the difference of the patterns, $y_{\text{obs}} - y_{\text{cal}}$. The blue lines at the bottom indicate the allowed Bragg reflections.

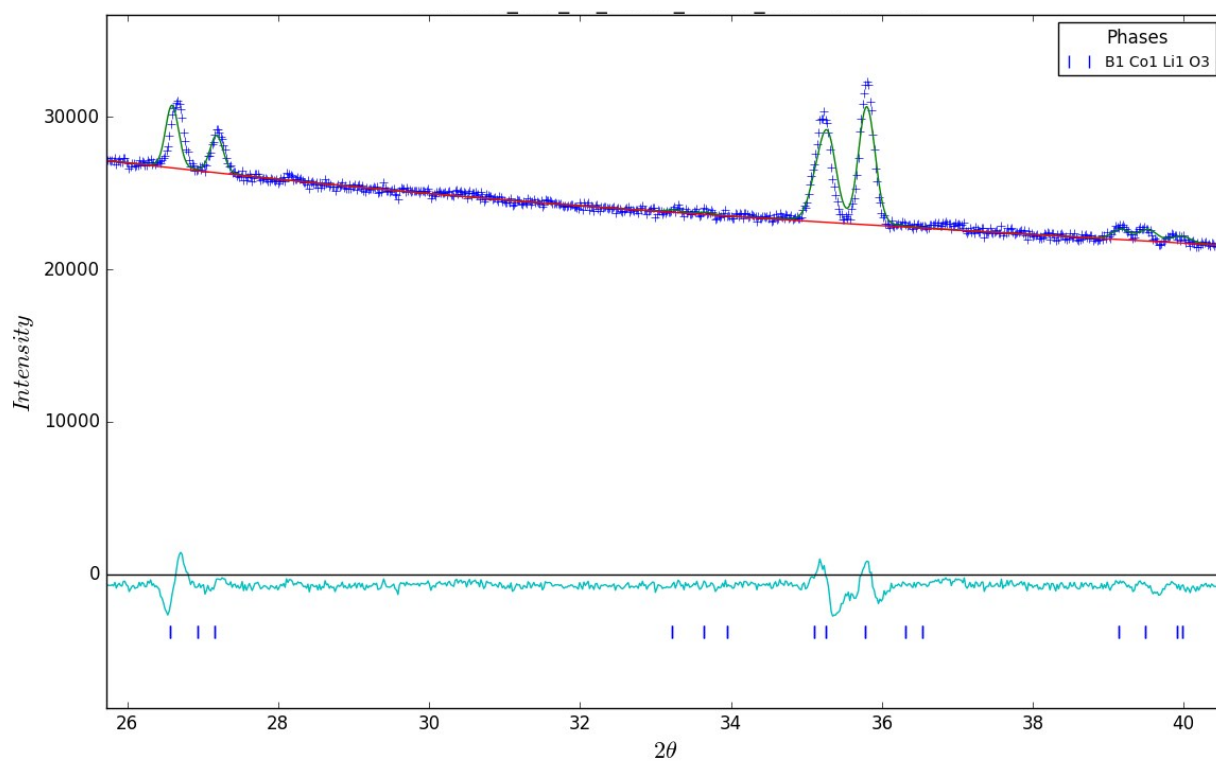


Figure S1 Supplement Zoomed in region from the refinement (Figure S1) for $2\theta = 26$ and 41 degrees displaying the quality of the fit. The blue curve corresponds to the experimental data and the green curve is the calculated fit. The bottom cyan coloured curve is the difference of the patterns, $y_{obs} - y_{cal}$. The blue lines at the bottom indicate the allowed Bragg reflections.

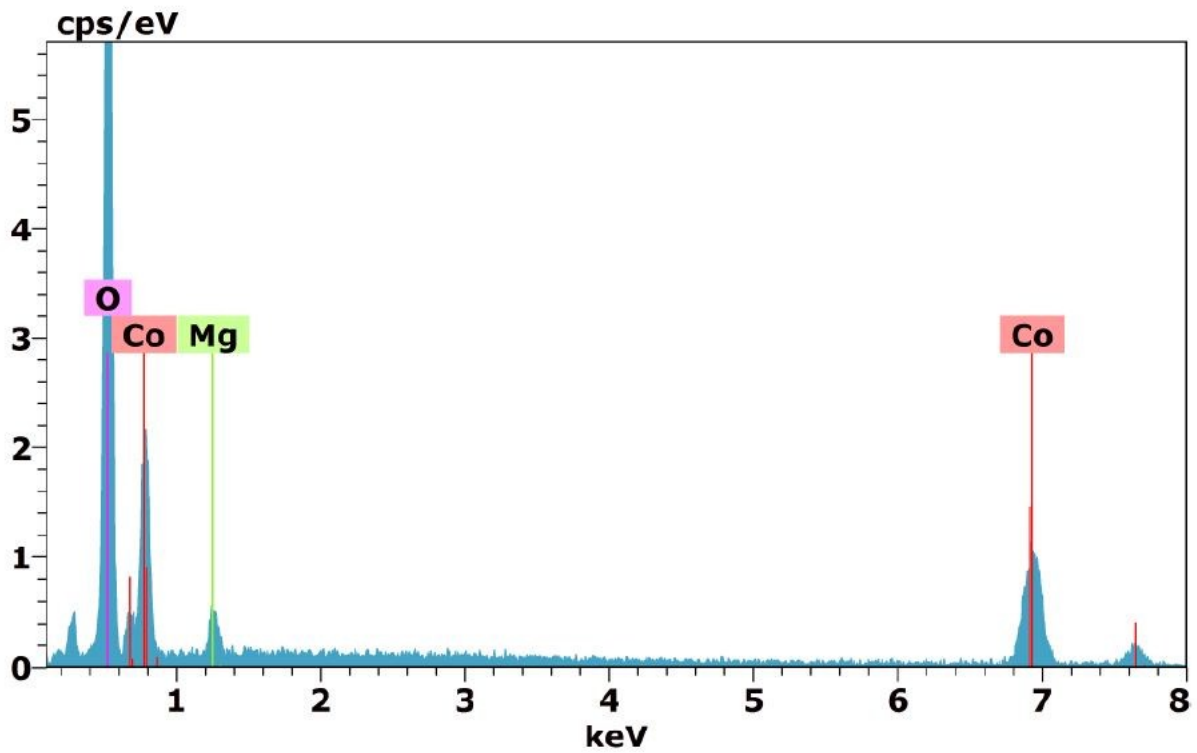


Figure S 2 EDX analysis result showing the characteristic energies of K_{α} and L_{α} radiation of EDX detectable elements present in the active material.

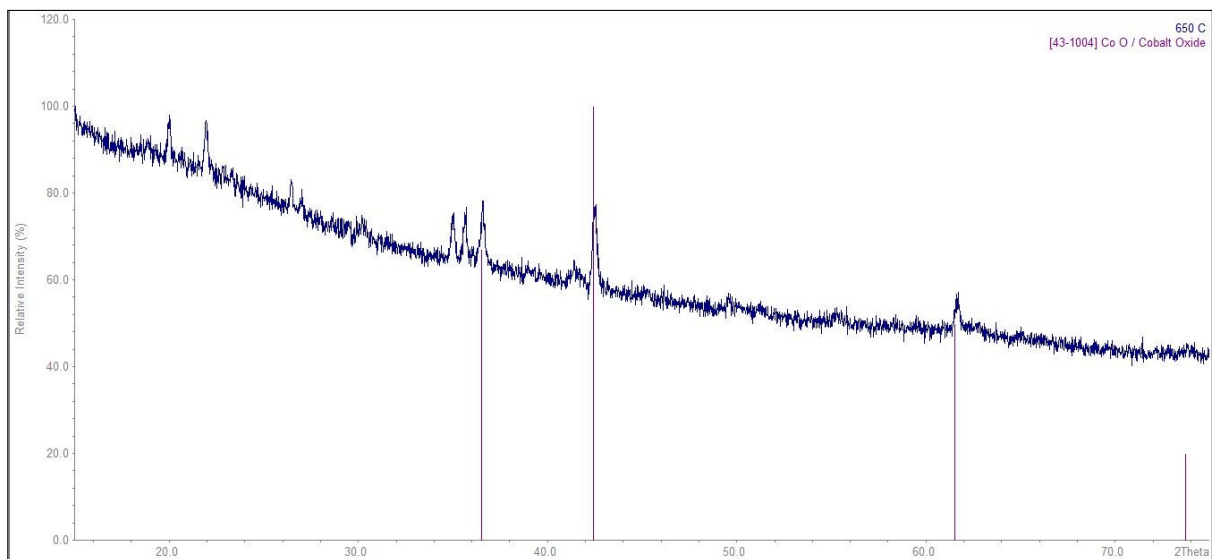


Figure S 3 XRD powder diagram showing the presence of CoO (PDF #43-1004) impurity peaks after annealing the gel-powder at 650 °C.

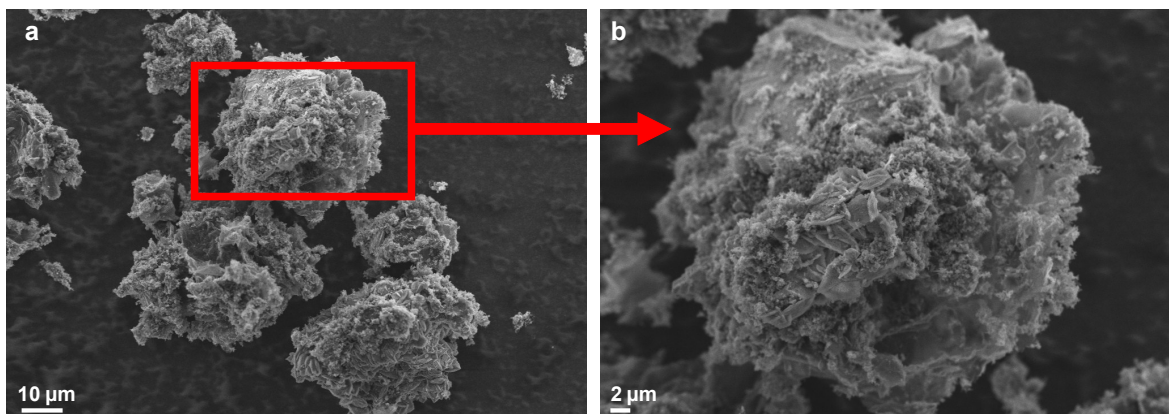


Figure S 4 The SEM micrographs of the active material ($\text{LiMg}_{0.1}\text{Co}_{0.9}\text{BO}_3$) after mixing with conductive carbon, reduced graphite oxide, and PVDF show that the material was completely coated and had a textured surface.

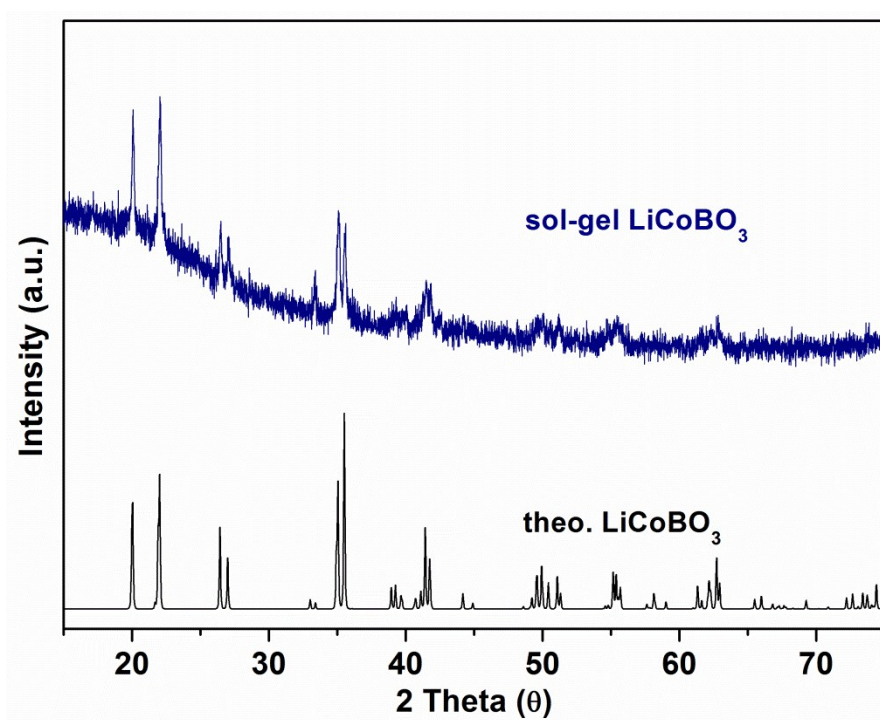


Figure S 5 XRD powder patterns of sol-gel synthesised LiCoBO_3 (blue) and calculated (ICSD 59346) LiCoBO_3 (black).

The XRD powder pattern of the sol-gel synthesised LiCoBO_3 obtained in similar conditions to $\text{LiMg}_{0.1}\text{Co}_{0.9}\text{BO}_3$ (e.g. the gel-powder annealed above $750\text{ }^\circ\text{C}$) is shown in **Figure S5**. The experimental pattern could be directly matched to the calculated one and no obvious impurity

phases that would affect the electrochemical performance of the active material can be observed.

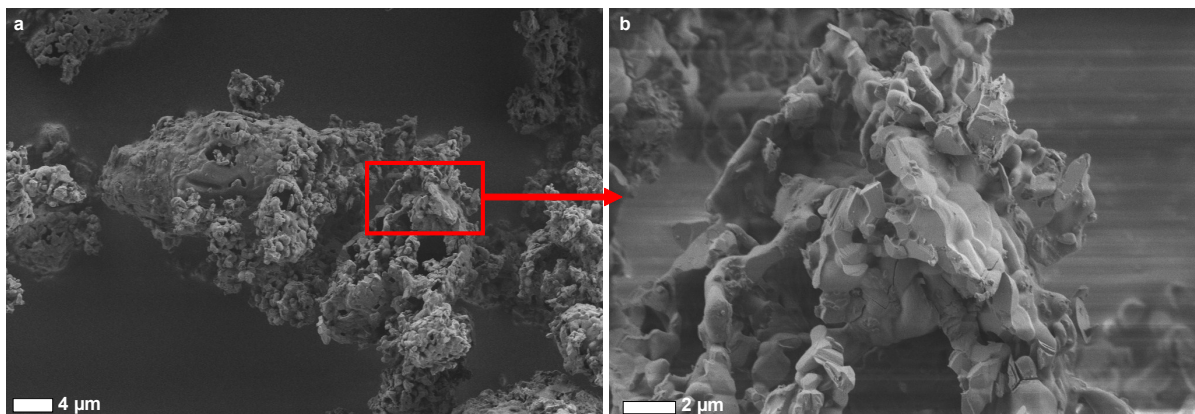


Figure S 6 The SEM micrographs of the sol-gel synthesised LiCoBO_3 .

The SEM micrographs of the sol-gel synthesised LiCoBO_3 is shown in Figure S6. The material was obtained by annealing the gel-powder at ~ 750 °C similar to the case of $\text{LiMg}_{0.1}\text{Co}_{0.9}\text{BO}_3$. The micron sized particles can be observed in the SEM images and appear form larger agglomerates.

References

1. B. H. Toby and R. B. Von Dreele, *J Appl Crystallogr*, 2013, **46**, 544-549.
2. Y. Piffard, K. K. Rangan, Y. L. An, D. Guyomard and M. Tournoux, *Acta Crystallogr C*, 1998, **54**, 1561-1563.